Spontaneous Hall effect enhanced by local Ir moments in epitaxial Pr_{2}Ir_{2}O_{7} thin films

Lu Guo, Neil Campbell, Yongseong Choi, Jong-Woo Kim, Philip J. Ryan, Huaixun Huyan, Linze Li, Tianxiang Nan, Jong-Hong Kang, Chris Sundahl, Xiaoqing Pan, M. S. Rzchowski, and Chang-Beom Eom

Phys. Rev. B **101**, 104405 — Published 5 March 2020

DOI: 10.1103/PhysRevB.101.104405

Spontaneous Hall Effect enhanced by local Ir moments in epitaxial $Pr_2Ir_2O_7$ thin films

Lu Guo,[1] Neil Campbell,[2] Yongseong Choi,[3] Jong-Woo Kim,[3] Philip J. Ryan,[3,6] Huaixun Huyan,[4] Linze Li,[4] Tianxiang Nan,[1] Jong-Hong Kang,[1] Chris Sundahl,[1] Xiaoqing Pan,[4,5,7] M.S. Rzchowski,[2] Chang-Beom Eom[1*]

[1]Department of Materials Science and Engineering, University of Wisconsin-Madison, Madison, Wisconsin 53706, USA

[2]Department of Physics, University of Wisconsin-Madison, Madison, Wisconsin 53706, U6SA

[3]Advanced Photon Source, Argonne National Laboratory, Argonne, Illinois 60439, USA

[4]Department of Materials Science and Engineering, University of California, Irvine, California 92697, USA

[5]Department of Physics and Astronomy, University of California, Irvine, California 92697, USA

[6]School of Physical Sciences, Dublin City University, Dublin 9, Ireland

[7]Irvine Materials Research Institute, University of California, Irvine, CA 92697, USA

Rare earth pyrochlore Iridates ($RE_2Ir_2O_7$) consist of two interpenetrating cation sublattices, the *RE* with highly-frustrated magnetic moments, and the Iridium with extended conduction orbitals significantly mixed by spin-orbit interactions. The coexistence and coupling of these two sublattices create a landscape for discovery and manipulation of quantum phenomena such as the topological Hall effect, massless conduction bands, and quantum criticality. Thin films allow extended control of the material system via symmetry-lowering effects such as strain. While bulk $Pr_2Ir_2O_7$ shows a spontaneous hysteretic Hall effect below 1.5K, we observe the effect at elevated temperatures up to 15K in epitaxial thin films on (111) YSZ substrates synthesized via solid phase epitaxy. Similar to the bulk, the lack of observable long-range magnetic order in the thin films points to a topological origin. We use synchrotron-based element-specific x-ray diffraction (XRD) and x-ray magnetic circular dichroism (XMCD) to compare powders and thin films to attribute the spontaneous Hall effect in the films to localization of the Ir moments. We link the thin film Ir local moments to lattice distortions absent in the bulk-like powders. We conclude that the elevated-temperature spontaneous Hall effect is caused by the topological effect originating either from the Ir or Pr sublattice, with interaction strength enhanced by the Ir local moments. This spontaneous Hall effect with weak net moment highlights the effect of vanishingly small lattice distortions as a means to discover topological phenomena in metallic frustrated magnetic materials.

*eom@engr.wisc.edu

Rare-Earth pyrochlore Iridates have been the subject of much research interest as a result of predictions and observations of phenomena such as bulk and edge massless conduction, frustrated magnetism, and metal-insulator transitions[1–5]. The key to the intriguing properties of $RE_2Ir_2O_7$ is the intimate coupling of two disparate sublattices of ionic *RE* and conducting Ir cations, as well as connecting oxygens. Each sublattice consists of alternating triangular and Kagome planes that are more easily visualized as forming a corner-sharing tetrahedra network (Fig. 1(a)). The high coordination of the lattice allows significant overlap of Ir orbitals simultaneous with frustrated magnetism of the *RE* ions.

The *RE* magnetic exchange interactions are mediated by the conducting Ir bands through the RKKY interaction[4]. As a result of the lattice geometry and antiferromagnetic nearest-neighbor coupling, spins on the *RE* and Ir sublattices are constrained to point toward or away from the center of one of the adjacent tetrahedra, forming frustrated spin-liquid correlations as examples are shown in Fig. 1(b)-(c). The *RE* ions have typical local moments of a few Bohr magnetons[4], while the Ir ions have a smaller moment which can be local or delocalized[6,7]. Ir adds to the complexity due to its strong spin-orbit coupling, mixing together the orbital and spin degrees of freedom.

In the $RE_2Ir_2O_7$ family, bulk $Pr_2Ir_2O_7$ is unique in that it is metallic down to the lowest temperatures and shows topological Hall effect below 1.5K as a result of various two-in-two-out magnetic configurations at the Pr sites with no net magnetic moment or long-range order. Furthermore, in thin films this topological Hall effect was observed at elevated temperatures up to 50K[8]. While there has been speculation about the role of Ir in this effect[8], here we combine Hall measurements, synchrotron X-ray diffraction and spectroscopy techniques to provide direct evidence supporting the emergence of Ir local moments, induced by the vanishingly small lattice modification of the Ir sublattice in the epitaxial $Pr_2Ir_2O_7$ thin films. We show a definitive link between the emergence of Ir local moments, which are absent in bulk $Pr_2Ir_2O_7$, and the increased onset temperature of the spontaneous Hall effect in the films.

To study the Hall effect in $Pr_2Ir_2O_7$ thin films, we synthesized stoichiometric epitaxial relaxed films via the solid-phase-epitaxy method, see supplemental information for details[9]. The high resolution Scanning Transmission Electron Microscopy (STEM) image across the interface between the film and substrate, as shown in Fig. 2(g), together with X-ray diffraction in Fig. 2(a)-(f), confirms a good epitaxial relationship and a sharp interface. Moreover, the modulated intensity contrast in Fig. 2(g) arises from an atomic number modulation between columns, indicating an atomic arrangement in the film that matches the ordered pyrochlore lattice. Energy Dispersive x-ray Spectroscopy (EDS) confirms the cation ratio between Pr and Ir is almost 1:1 (Fig. S1(g)). While the pyrochlore structure is nominally cubic, the synchrotron X-ray diffraction study shows different d-spacing for the (6 0 10) and (0 $\bar{6}$ 10) reflections, which are equivalent under cubic symmetry. This points toward a breaking of the cubic symmetry in our epitaxial $Pr_2Ir_2O_7$ thin film; however, the distortion is too small for us to discern the specific symmetry of the lattice from the X-ray diffraction study (see supplemental Table S1[9]). There are indications

that a trigonal distortion of the Ir sublattice can change the electronic and magnetic properties of $Pr_2Ir_2O_7$[10]. However our result pushes the lower limit of the lattice distortion necessary to effectively alter the Ir local electronic environment enough to produce the spontaneous Hall enhancement.

We use Hall measurements to study the electronic and magnetic manifestations of minor lattice distortions in the epitaxial $Pr_2Ir_2O_7$ films. Fig. 3(b) shows the Hall signal at different temperatures with applied magnetic field along the [111] direction. At temperatures below 20K, the Hall conductivity is non-linear, becomes hysteretic, and develops a small remnant value at zero field, referred to here as the spontaneous Hall effect. A similar effect is observed in the bulk single crystal, but only at temperatures an order of magnitude lower[3,8]. The origin of such effect most commonly occurs from a spontaneous net magnetic moment via the anomalous Hall effect. We rule out this contribution based on our x-ray measurements, which indicate the net Ir moment is less than 0.05μB/Ir at 5 T and the film lacks long-range magnetic ordering (Fig. S2). Consequently, we conclude that the spontaneous Hall effect in the film arises from the topological Hall effect. In this case, as discussed in the supplementary information[9], the time-reversal symmetry is broken from the frustrated spin-liquid correlations rather than a net magnetic moment.

Since the *RE* and Ir cations are both magnetically active, we use element-resolved x-ray magnetic scattering and spectroscopy to explore the individual Pr and Ir sublattice contributions to the spontaneous Hall effect. X-ray resonant diffraction measurements at the Ir L_3 edge of our thin films from 65K down to 5K, covering the temperature regime above and below the observed onset of the spontaneous Hall effect, show no clear indications of any type of long-range magnetic ordering (Fig. S6-S7) including Ir-site AIAO ordering, consistent with the intrinsic bulk single-crystal behavior.

To help us understand the $Pr_2Ir_2O_7$, we compare the Pr L_2-XMCD results of our thin film with that of cubic-symmetric $Pr_2Ir_2O_7$ powders. Comparison of film Pr L_2-XMCD peaks (Fig. 4) and the reference powder peaks (Fig. S3) suggests that Pr spins behave identically in films and powders. In addition, the field dependence of the Pr L_2-XMCD signal from the film (Fig. S4(a)) resembles the magnetometry result from the powder sample (Fig. S2(a)). These results suggest that the structural distortion in the film does not modify the Pr magnetism. This makes sense as the Pr 4*f* orbitals are fairly localized and overlap less with the distorted surrounding atoms. This contrasts sharply with the Ir 5*d* orbitals that are much more dispersive and so more susceptible to structural distortion effects. Previous studies have shown that distortion of the IrO_6 octahedra in perovskite iridate superlattices induces long-range magnetic ordering and an insulating ground state[11].

To investigate potential changes in the Ir magnetism in the films, we compared the Ir $L_{2,3}$ XAS and XMCD data from the $Pr_2Ir_2O_7$ film with $Pr_2Ir_2O_7$ and Sr_2IrO_4 powders. As shown in Fig. 5 and supplemental Fig. S5, the absorption edge positions and the L_3/L_2 branching ratios are similar for both powders, as well as the film, and also with previously studied

$SrIrO_3/La_{0.3}Sr_{0.7}MnO_3$[7], confirming large spin-orbit coupling and a Ir^{4+} electronic environment in all materials[12]. Despite the similarity of the Ir orbital state, the XMCD signal under 5T on $Pr_2Ir_2O_7$ powders at the Ir L_3 edge is less than 10% of that in Sr_2IrO_4 powders. The observed weak Ir-XMCD value is expected due to the lack of long-range ordering on the Ir 5*d* moments[3]. Furthermore, the Ir-XMCD results here differ significantly from the cases related to spin-orbit coupled Ir local moments with strong orbital magnetic moments[6,7]. Unexpectedly, the Ir-L_3 XMCD sign from the $Pr_2Ir_2O_7$ powder indicates that the Ir induced moments are anti-parallel to the external field, in sharp contrast to the Sr_2IrO_4 case, which shows long-range ordered moments with a net moment of 0.05 μ_B/Ir[6]. Disparate Ir-L_2 XMCD signals seen in these powder samples provide clues to understand the discrepancy in the Ir-L_3 XMCD signals and the overall magnetism in these two materials. Whereas the negligible Ir-L_2 XMCD signal (in comparison with the L_3 signal) from the Sr_2IrO_4 is the characteristic signature of the J_{eff}=1/2 state, the $Pr_2Ir_2O_7$ powders show comparable amplitudes with opposite signs between the Ir L_2 and L_3 edges. This reveals that the observed Ir spin moments in the $Pr_2Ir_2O_7$ powder samples originate from small spin polarization in the conduction band by Pr moments, distinctively different from localized Ir moments in the Sr_2IrO_4 case. This is in accordance with resistivity results which suggest small conduction electron magnetization via the Kondo effect as shown in Fig. 3(a).

We now discuss the difference between $Pr_2Ir_2O_7$ film and powders, in particular that our XMCD data show a magnetically active Ir sublattice in the film, as opposed to the weak polarization of the Ir spins we observed in powders. The Ir-XMCD signals in the film are an order of magnitude larger than in the $Pr_2Ir_2O_7$ powder, indicating a field-induced alignment of local Ir moments, as shown in Fig. 5. The sign of Ir-L_3 XMCD in the $Pr_2Ir_2O_7$ thin film, contrary to that of the $Pr_2Ir_2O_7$ powders, indicates that the net Ir moment aligns with the external field, and thus is parallel to the Pr 4*f* net moment. Moreover, the much smaller XMCD signal at the L_2 edge relative to L_3 suggests that, unlike the $Pr_2Ir_2O_7$ powder, the Ir 5*d* electronic state in the $Pr_2Ir_2O_7$ thin film is close to the J_{eff} = 1/2 state which is observed in Sr_2IrO_4[6,7]. We thus conclude that the vanishingly-small structural distortion present in our thin films has a profound impact on the electronic properties by localizing the Ir moments and changing the Ir t_{2g} manifold toward the J_{eff} = 1/2 observed in other iridates[13].

Our findings are also consistent with the theoretical predictions that a trigonal distortion of the Ir sublattice can enhance the formation of Ir local moments[14]. Previous theoretical work suggested a trigonal distortion of the Ir sublattice can affect the octahedral crystal field and result in non-trivial topological phases in $RE_2Ir_2O_7$ by stabilizing the AIAO spin configuration at Ir sites[10]. Our results highlight the disproportionate effect of a trivial lattice distortion on the Ir sublattice inducing incipient Ir 5d local moments as a manifestation of perturbations to the t_{2g} bands[15].

Previous work notes that the Pr-Pr interaction strength is too weak to allow chiral spin liquid correlations on the Pr sublattice at temperatures above 1.5K, despite measurable spontaneous Hall effect signal. The origin of the observed effect was attributed to broken time reversal symmetry at the Ir sublattice[8]. As the most similar point of comparison to $Pr_2Ir_2O_7$ is

$Nd_2Ir_2O_7$, which shows AIAO spin ordering at both the Nd and Ir sites in the insulating phase[16], Ohtsuki et al propose AIAO to be the most likely configuration for Ir in $Pr_2Ir_2O_7$[8]. The AIAO ordering and its relationship to the A site elements have been well linked throughout the rare earth pyrochlore iridate series (apart from Pr), with neutron scattering and resonant elastic and inelastic x-ray scattering[16–19]. But we did not observe any signal that would indicate long-range AIAO ordering in the Ir sublattice (Fig. S6-S7).

As a result of not observing Ir-AIAO ordering, we consider other ways in which Ir moments play a role in the observed TRS breaking. One possible mechanism is that the Ir local moments, having the same frustrated lattice structure as the Pr, form the same chiral spin liquid correlations, just at higher temperatures. The spontaneous Hall effect in bulk $Pr_2Ir_2O_7$ has been attributed to altering dominant 3-in/out-1-out/in and 2-in-2-out correlations variants at the Pr sites, which leads us to presume these same correlations at the Ir sites can produce the spontaneous Hall effect. This is consistent with the Ir-site spin correlations preceding the Pr-site correlations with cooling, as observed in $RE_2Ir_2O_7$ materials through their MIT. In this scenario, the observed small Ir net moment, presumably from canting or defects, couples with the external field, allowing the external field to manipulate the Ir-site spin liquid correlations while not directly producing the anomalous Hall effect[20].

A second possible mechanism is that the Ir local moments renormalize the effective Pr-Pr interaction strength, raising the temperature of the spin-liquid correlation onset of the Pr moments. Since the RKKY interaction describes the Pr-Pr coupling as mediated by the Ir conduction band, consistent with AFM coupling and nonzero conductivity, spin polarization at the Ir site should impact this interaction. Subsequently, on the basis of drastically different conduction properties of the Pr and Ir sublattices, one would expect Ir-site spin-liquid correlations to manifest differently in the spontaneous Hall effect than the Pr-site correlations. Yet despite this, the spontaneous Hall effect hysteresis loops appear very similar to the bulk loops attributed to Pr-site correlations[3]. In this scenario, the Ir sublattice would maintain no chiral spin-liquid correlations at all temperatures, and the Ir TRS breaking would only indirectly contribute to the spontaneous Hall effect. The Pr sublattice chiral spin liquid correlations would be the 2-in-2-out and 3-in/out-1-out/in correlations responsible for the spontaneous Hall effect in the bulk[3]. In $Eu_2Ir_2O_7$ films (with no magnetic contribution from Eu^{3+} ions), anomalous Hall effect has been observed, highlighting the contribution of magnetic Ir ions[21]. At this point our experimental evidence does not rule out either scenario, and future studies on the $RE_2Ir_2O_7$ (without *RE* local moment) may shed further light on the role of the magnetic Ir sublattice in the Hall effect.

In conclusion, we observed that small lattice distortions in $Pr_2Ir_2O_7$ thin films act as a perturbation, changing the local magnetic properties of the Ir sublattice and inducing a spontaneous Hall effect at elevated temperatures. By analyzing the XMCD signal at the Pr and Ir *L* edges, we attribute the enhanced spontaneous Hall response in the thin films to localized net moments on the Ir sublattice. Our observations reveal the possible link between structural change in the Ir network, the Ir local magnetic environment, and transport behavior. Understanding these

effects provides opportunities to manipulate the 5*d* pyrochlore iridate ground states by modifying the lattices, making this system attractive as a promising candidate in spintronics. Our work opens up new possibilities for controlling electronic and magnetic phenomena in conducting frustrated antiferromagnets via thin-film epitaxy.

Acknowledgements

Synthesis of thin films at the University of Wisconsin-Madison was supported by NSF through the University of Wisconsin Materials Research Science and Engineering Center (DMR-1720415) and DMREF (Grant No. DMR-1629270). Transport and magnetic measurements at the University of Wisconsin-Madison was supported by the US Department of Energy (DOE), Office of Science, Office of Basic Energy Sciences, under award number DEFG02-06ER46327. X-ray diffraction and absorption experiments were carried out at beamlines 6-ID-B and 4-ID-D of the Advanced Photon Source, Argonne National Laboratory. The work performed at the Advanced Photon Source was supported by the U.S. Department of Energy, Office of Science, and Office of Basic Energy Sciences under Contract No. DEAC02-06CH11357. TEM experiments were conducted using the advanced TEM facilities in the Irvine Materials Research Institute (IMRI) at the University of California, Irvine.

References

[1] T. Kondo, M. Nakayama, R. Chen, J.J. Ishikawa, E.-G. Moon, T. Yamamoto, Y. Ota, W. Malaeb, H. Kanai, Y. Nakashima, Y. Ishida, R. Yoshida, H. Yamamoto, M. Matsunami, S. Kimura, N. Inami, K. Ono, H. Kumigashira, S. Nakatsuji, L. Balents, and S. Shin, Nat. Commun. **6**, 10042 (2015).

[2] B. Cheng, T. Ohtsuki, D. Chaudhuri, S. Nakatsuji, M. Lippmaa, and N.P. Armitage, Nat. Commun. **8**, 2097 (2017).

[3] Y. MacHida, S. Nakatsuji, S. Onoda, T. Tayama, and T. Sakakibara, Nature **463**, 210 (2010).

[4] S. Nakatsuji, Y. Machida, Y. Maeno, T. Tayama, T. Sakakibara, J. van Duijn, L. Balicas, J.N. Millican, R.T. Macaluso, and J.Y. Chan, Phys. Rev. Lett. **96**, 087204 (2006).

[5] K. Matsuhira, M. Wakeshima, Y. Hinatsu, and S. Takagi, J. Phys. Soc. Japan **80**, 094701 (2011).

[6] D. Haskel, G. Fabbris, M. Zhernenkov, P.P. Kong, C.Q. Jin, G. Cao, and M. van Veenendaal, Phys. Rev. Lett. **109**, 027204 (2012).

[7] J.-W. Kim, Y. Choi, S.H. Chun, D. Haskel, D. Yi, R. Ramesh, J. Liu, and P.J. Ryan, Phys. Rev. B **97**, 094426 (2018).

[8] T. Ohtsuki, Z. Tian, A. Endo, M. Halim, S. Katsumoto, Y. Kohama, K. Kindo, M. Lippmaa, and S. Nakatsuji, Proc. Natl. Acad. Sci. **116**, 8803 (2019).

[9] see supplementary materials.

[10] B.-J. Yang and Y.B. Kim, Phys. Rev. B **82**, 085111 (2010).

[11] J. Matsuno, K. Ihara, S. Yamamura, H. Wadati, K. Ishii, V. V. Shankar, H.-Y. Kee, and H. Takagi, Phys. Rev. Lett. **114**, 247209 (2015).

[12] G. van der Laan and B.T. Thole, Phys. Rev. Lett. **60**, 1977 (1988).

[13] J.W. Kim, Y. Choi, J. Kim, J.F. Mitchell, G. Jackeli, M. Daghofer, J. van den Brink, G. Khaliullin, and B.J. Kim, Phys. Rev. Lett. **109**, 037204 (2012).

[14] Y. Wang, H. Weng, L. Fu, and X. Dai, Phys. Rev. Lett. **119**, 187203 (2017).

[15] D. Uematsu, H. Sagayama, T.-H. Arima, J.J. Ishikawa, S. Nakatsuji, H. Takagi, M. Yoshida, J. Mizuki, and K. Ishii, Phys. Rev. B **92**, 094405 (2015).

[16] K. Tomiyasu, K. Matsuhira, K. Iwasa, M. Watahiki, S. Takagi, M. Wakeshima, Y. Hinatsu, M. Yokoyama, K. Ohoyama, and K. Yamada, J. Phys. Soc. Japan **81**, 034709 (2012).

[17] H. Sagayama, D. Uematsu, T. Arima, K. Sugimoto, J.J. Ishikawa, E. O'Farrell, and S. Nakatsuji, Phys. Rev. B **87**, 100403(R) (2013).

[18] C. Donnerer, M.C. Rahn, M.M. Sala, J.G. Vale, D. Pincini, J. Strempfer, M. Krisch, D. Prabhakaran, A.T. Boothroyd, and D.F. McMorrow, Phys. Rev. Lett. **117**, 037201 (2016).

[19] Z. Porter, E. Zoghlin, S. Britner, S. Husremovic, J.P.C. Ruff, Y. Choi, D. Haskel, G. Laurita,

and S.D. Wilson, Phys. Rev. B **100**, 054409 (2019).

[20] S. Nakatsuji, N. Kiyohara, and T. Higo, Nature **527**, 212 (2015).

[21] T.C. Fujita, Y. Kozuka, M. Uchida, A. Tsukazaki, T. Arima, and M. Kawasaki, Sci. Rep. **5**, 9711 (2015).

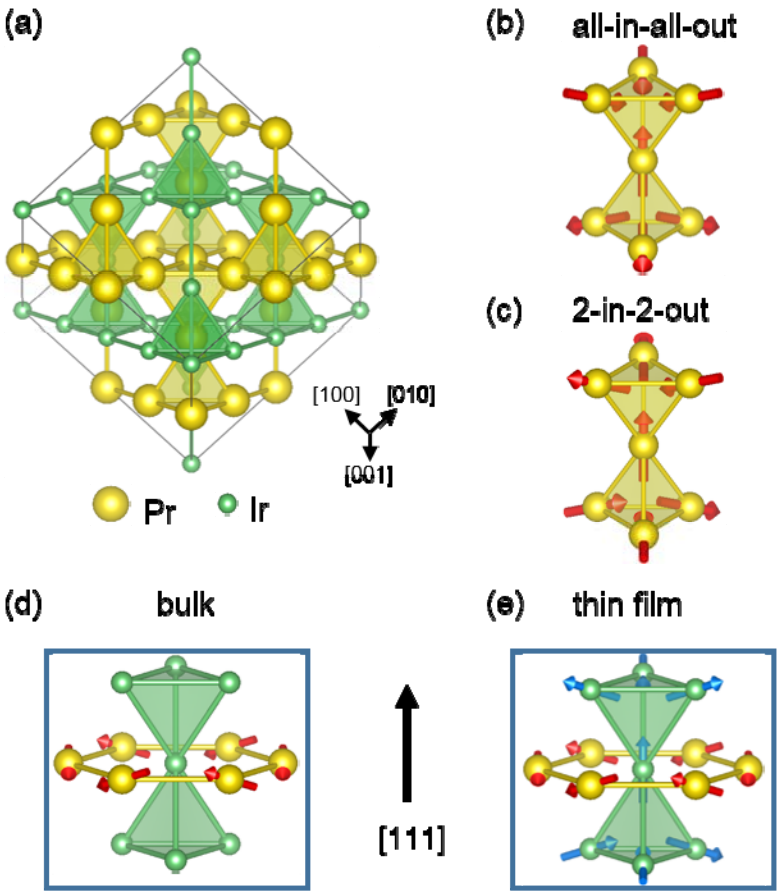

Figure 1: (a) Unit cell of $Pr_2Ir_2O_7$ with only cation sublattices shown. Oxygen atoms are not shown for clarity. (b, c) 'All-in-all-out' and '2-in-2-out' spin configurations on the Pr corner sharing tetrahedra. (d, e) Zoom-in of corner-sharing Ir tetrahedral surrounded by Pr hexagonal ring in the (111) plane of the bulk and thin film respectively. The red arrows in the Pr atoms indicate the Pr 4f moments. Due to the cubic symmetry-breaking in the thin film, Ir local moments can be established indicated here in (e) by the blue arrows in Ir atoms.

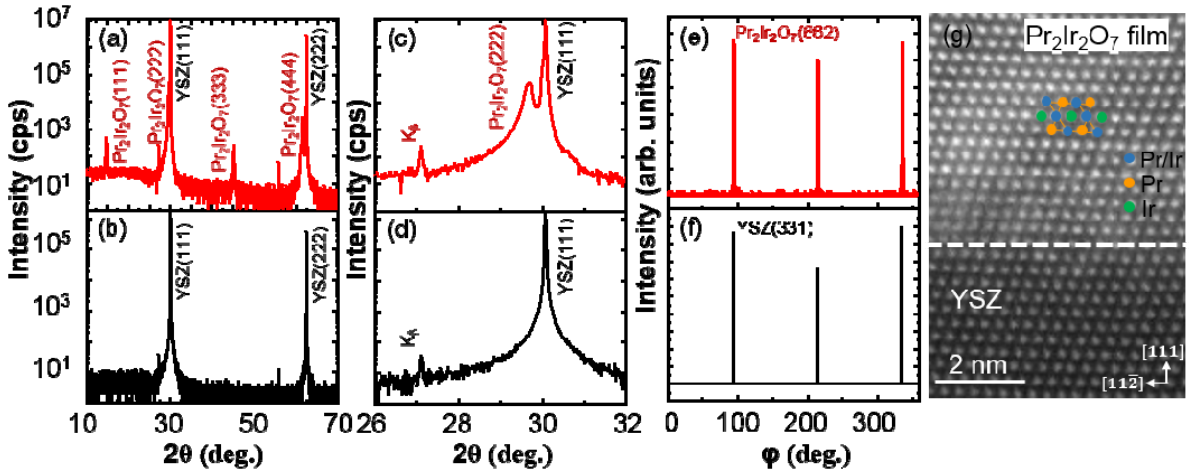

Figure 2: Out-of-plane 2θ-ω scan of (a) the post-annealed and (b) the as-grown film. Zoom-in out-of-plane 2θ-ω scan near YSZ (111) peak of (c) the post-annealed and (d) the as-grown film. The peak at 27^0 in both scans are reflections from substrate with Cu K_β wavelength. Phi-scan patterns of the (e) {662} planes from the epitaxial crystalline $Pr_2Ir_2O_7$ thin film and (f) {331} planes from the YSZ (111) substrate. (g) Cross-sectional HRSTEM image across the interface between epitaxial $Pr_2Ir_2O_7$ thin film and (111) YSZ substrate. The Pr, and Ir atomic positions labeled in the selected areas are consistent with pyrochlore structure. The blue dots represent the mixed Pr and Ir column due to the alternating arrangement along zone axis. The O atoms are omitted.

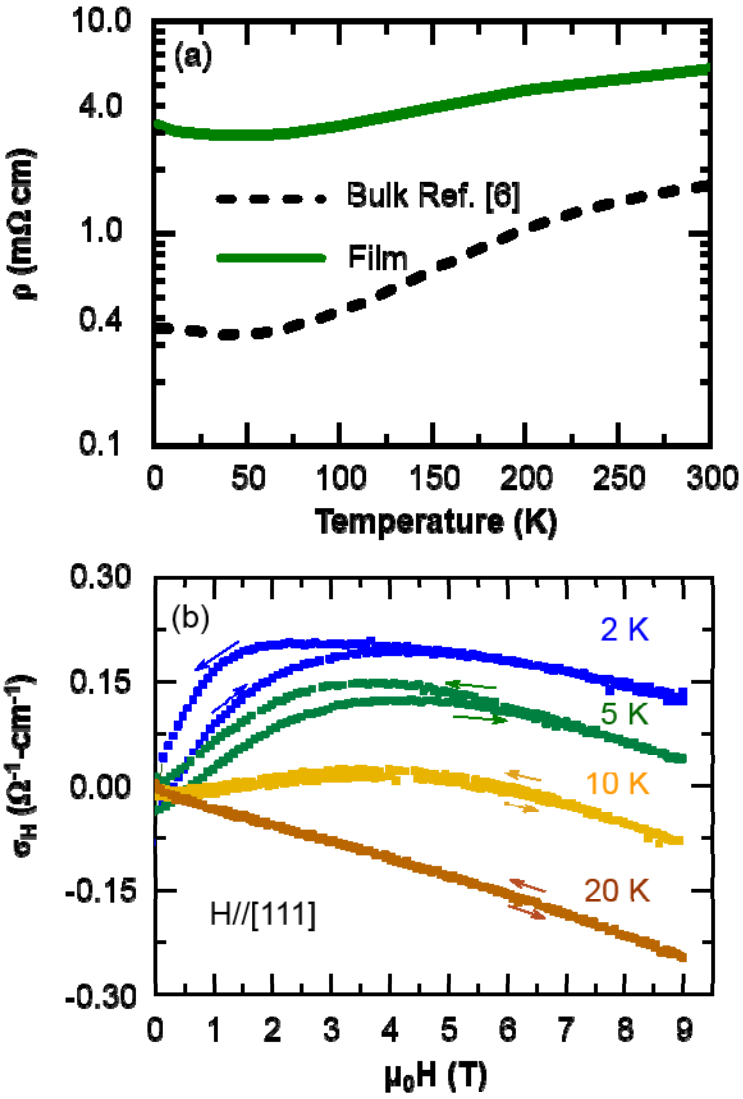

Figure 3: (a) Temperature dependence of the longitudinal resistivity of the epitaxial $Pr_2Ir_2O_7$ thin film (solid green line) and the bulk $Pr_2Ir_2O_7$ single crystal (black dashed line) from Ref. 6. (b) Hall conductivity as a function of external out-of-plane magnetic field at different temperatures.

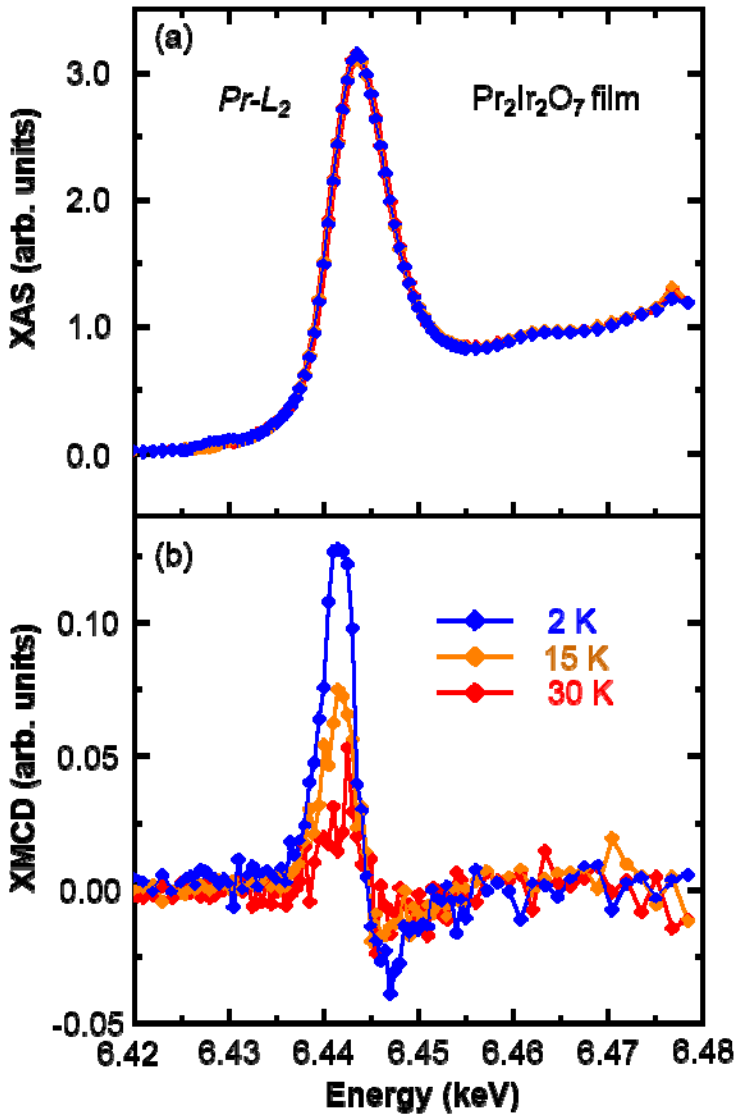

Figure 4: (a) XAS and (b) XMCD spectra at the Pr L_2 edge under 5T magnetic field (along [111] direction) on $Pr_2Ir_2O_7$ thin films through the spontaneous Hall effect transition.

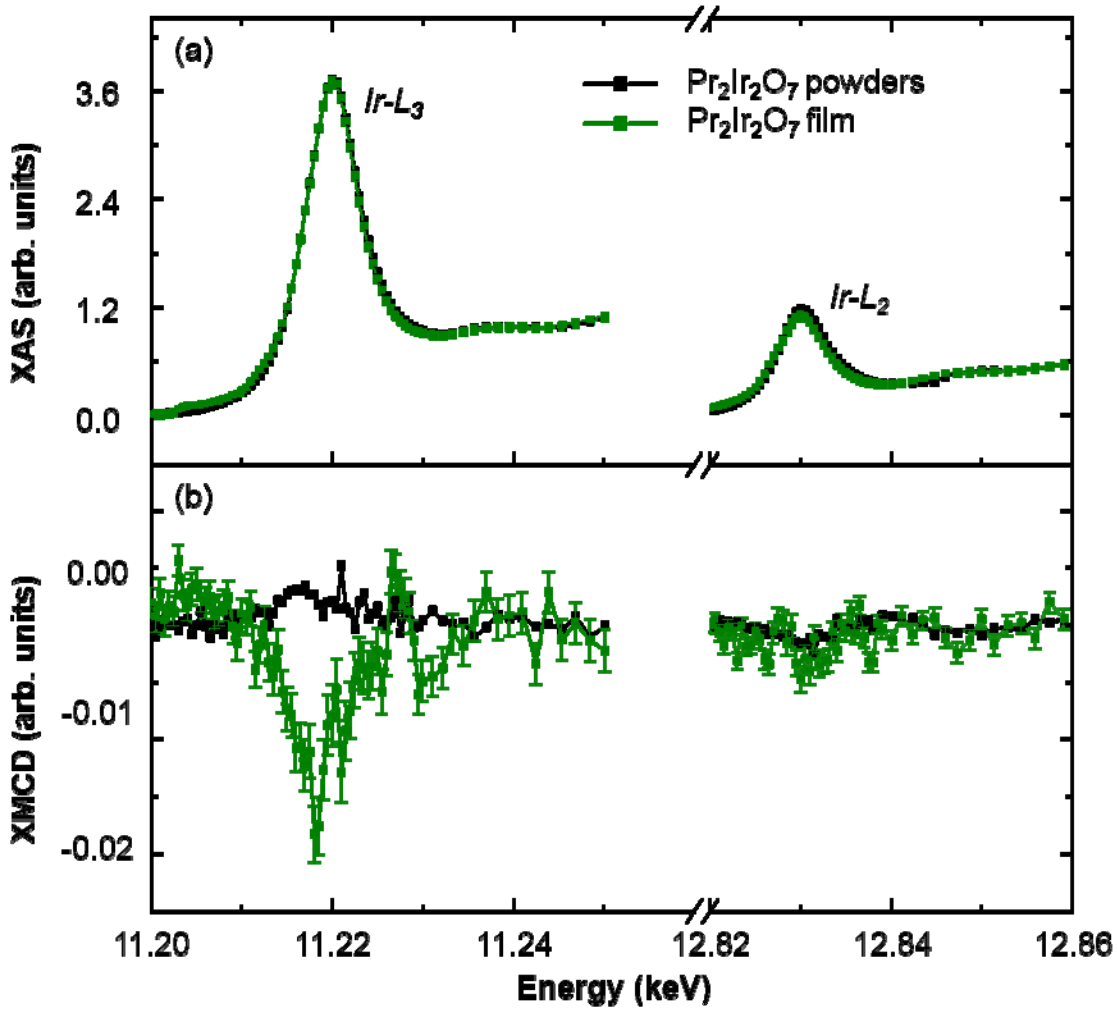

Figure 5: The XAS and the XMCD spectra at 2K under 5T with magnetic field along the [111] direction at the Ir $L_{2,3}$ edges are compared between the $Pr_2Ir_2O_7$ film (green) and $Pr_2Ir_2O_7$ reference powders (black). The field direction was along the [111] direction of the film sample. For the powder case, the measurement is sensitive to the net Ir moment averaged over the randomly oriented grains.